Defense Threat Reduction Agency
8725 John J. Kingman Road, MS
6201 Fort Belvoir, VA 22060-6201

DTRA-TR-18-54

TECHNICAL REPORT

Source Parameter Estimation using the Second-order Closure Integrated Puff Model

May 2018

HDTRA01-13-C-0034

R. Ian Sykes et al.

Prepared by:
Sage Management
15 Roszel Road
Suite 102
Princeton, NJ 08543

DESTRUCTION NOTICE:

Destroy this report when it is no longer needed.
Do not return to sender.

PLEASE NOTIFY THE DEFENSE THREAT REDUCTION AGENCY, ATTN: DTRIAC/ RD-NTF, 8725 JOHN J. KINGMAN ROAD, MS-6201, FT BELVOIR, VA 22060-6201, IF YOUR ADDRESS IS INCORRECT, IF YOU WISH IT DELETED FROM THE DISTRIBUTION LIST, OR IF THE ADDRESSEE IS NO LONGER EMPLOYED BY YOUR ORGANIZATION.

REPORT DOCUMENTATION PAGE

Form Approved
OMB No. 0704-0188

1. REPORT DATE *(DD-MM-YYYY)*	**2. REPORT TYPE**	**3. DATES COVERED** *(From - To)*
00-05-2018	Technical	March 1, 2013 - March 1, 2016

4. TITLE AND SUBTITLE

Source Parameter Estimation using the Second-order Closure Integrated Puff Model

5a. CONTRACT NUMBER
HDTRA01-13-C-0034

5b. GRANT NUMBER

5c. PROGRAM ELEMENT NUMBER

6. AUTHOR(S)

R. Ian Sykes, B. Chowdhury, D.S. Henn

5d. PROJECT NUMBER

5e. TASK NUMBER

5f. WORK UNIT NUMBER

7. PERFORMING ORGANIZATION NAME(S) AND ADDRESS(ES)

Sage Management
15 Roszel Road
Site 102
Princeton, NJ 08543

8. PERFORMING ORGANIZATION REPORT NUMBER

9. SPONSORING / MONITORING AGENCY NAME(S) AND ADDRESS(ES)

Defense Threat Reduction Agency
8725 John J. Kingman Road, STOP 6201
Fort Belvoir, VA 22060-6201

10. SPONSOR/MONITOR'S ACRONYM(S)
DTRA

11. SPONSOR/MONITOR'S REPORT NUMBER(S)
DTRA-TR-18-54

12. DISTRIBUTION / AVAILABILITY STATEMENT

Distribution Statement A. Approved for public release; distribution is unlimited.

13. SUPPLEMENTARY NOTES

14. ABSTRACT

A new method for estimation of source parameters from sensor measurements, using the Second-order Closure Integrated Puff Model (SCIPUFF) is proposed. The sensor measurements are categorized as triggered and non-triggered based on the recorded concentration measurements and a threshold concentration value. Using each measured value, sources of adjoint material are created from the triggered and non-triggered sensors, and the adjoint transport equations are solved to predict the adjoint concentration fields. The adjoint source strength is inversely proportional to the concentration measurement for the sensor, and the adjoint source duration is equal to the averaging time of the sensor. Using the non-triggered adjoint concentrations at each location in the domain, each triggered adjoint concentration is weighted and the source release location is obtained by finding the location at which the triggered adjoint concentrations are closest to each other. Based on the release location, the release mass can also be ascertained. The method is tested using data from the Fusion Field Trial 2007 (FFT07) and the European Tracer Experiment (ETEX).

15. SUBJECT TERMS

Source Term Estimation, Reverse Transport Modeling, SCIPUFF, ETEX

16. SECURITY CLASSIFICATION OF:			**17. LIMITATION OF ABSTRACT**	**18. NUMBER OF PAGES**	**19a. NAME OF RESPONSIBLE PERSON**
a. REPORT	**b. ABSTRACT**	**c. THIS PAGE**			Dr. Ronald G. Meris
Unclassified	Unclassified	Unclassified	SAR	34	**19b. TELEPHONE NUMBER** *(include area code)* 703-767-2906

UNIT CONVERSION TABLE

U.S. customary units to and from international units of measurement*

U.S. Customary Units	Multiply by → / ← Divide by†		International Units
Length/Area/Volume			
inch (in)	2.54	$\times 10^{-2}$	meter (m)
foot (ft)	3.048	$\times 10^{-1}$	meter (m)
yard (yd)	9.144	$\times 10^{-1}$	meter (m)
mile (mi, international)	1.609 344	$\times 10^{3}$	meter (m)
mile (nmi, nautical, U.S.)	1.852	$\times 10^{3}$	meter (m)
barn (b)	1	$\times 10^{-28}$	square meter (m^2)
gallon (gal, U.S. liquid)	3.785 412	$\times 10^{-3}$	cubic meter (m^3)
cubic foot (ft^3)	2.831 685	$\times 10^{-2}$	cubic meter (m^3)
Mass/Density			
pound (lb)	4.535 924	$\times 10^{-1}$	kilogram (kg)
unified atomic mass unit (amu)	1.660 539	$\times 10^{-27}$	kilogram (kg)
pound-mass per cubic foot (lb ft^{-3})	1.601 846	$\times 10^{1}$	kilogram per cubic meter (kg m^{-3})
pound-force (lbf avoirdupois)	4.448 222		newton (N)
Energy/Work/Power			
electron volt (eV)	1.602 177	$\times 10^{-19}$	joule (J)
erg	1	$\times 10^{-7}$	joule (J)
kiloton (kt) (TNT equivalent)	4.184	$\times 10^{12}$	joule (J)
British thermal unit (Btu) (thermochemical)	1.054 350	$\times 10^{3}$	joule (J)
foot-pound-force (ft lbf)	1.355 818		joule (J)
calorie (cal) (thermochemical)	4.184		joule (J)
Pressure			
atmosphere (atm)	1.013 250	$\times 10^{5}$	pascal (Pa)
pound force per square inch (psi)	6.984 757	$\times 10^{3}$	pascal (Pa)
Temperature			
degree Fahrenheit (^oF)	$[T(^oF) - 32]/1.8$		degree Celsius (^oC)
degree Fahrenheit (^oF)	$[T(^oF) + 459.67]/1.8$		kelvin (K)
Radiation			
curie (Ci) [activity of radionuclides]	3.7	$\times 10^{10}$	per second (s^{-1}) [becquerel (Bq)]
roentgen (R) [air exposure]	2.579 760	$\times 10^{-4}$	coulomb per kilogram (C kg^{-1})
rad [absorbed dose]	1	$\times 10^{-2}$	joule per kilogram (J kg^{-1}) [gray (Gy)]
rem [equivalent and effective dose]	1	$\times 10^{-2}$	joule per kilogram (J kg^{-1}) [sievert (Sv)]

*Specific details regarding the implementation of SI units may be viewed at http://www.bipm.org/en/si/.

†Multiply the U.S. customary unit by the factor to get the international unit. Divide the international unit by the factor to get the U.S. customary unit.

CONTENTS

LIST OF FIGURES

LIST OF TABLES

SUMMARY

A new method for estimation of source parameters from sensor measurements, using the Second-order Closure Integrated Puff Model (SCIPUFF) is proposed. The sensor measurements are categorized as triggered and non-triggered based on the recorded concentration measurements and a threshold concentration value. Using each measured value, sources of adjoint material are created from the triggered and non-triggered sensors, and the adjoint transport equations are solved to predict the adjoint concentration fields. The adjoint source strength is inversely proportional to the concentration measurement for the sensor, and the adjoint source duration is equal to the averaging time of the sensor. Using the non-triggered adjoint concentrations at each location in the domain, each triggered adjoint concentration is weighted and the source release location is obtained by finding the location at which the triggered adjoint concentrations are closest to each other. Based on the release location, the release mass can also be ascertained. The method is tested using data from the Fusion Field Trial 2007 (FFT07) and the European Tracer Experiment (ETEX).

1 INTRODUCTION

The SCIPUFF model has been used for the atmospheric dispersion and hazard prediction in many applications, e.g. Sykes et al. (1993), Hanna et al. (2008), and is the main dispersion model in the operational US Department of Defense's Hazard Prediction and Assessment Capability (HPAC) system. In most cases, the source parameters are known and, together with meteorological information, these are used for the dispersion prediction and emergency response planning. However in some cases, such as in an accident or a terrorist attack involving a Chemical, Biological or Nuclear material, the actual source location or the source parameters may not be known. A sensor network in an urban or protected area can be triggered if concentration of the hazardous materials exceeds the alarm threshold. Using the sensor data, the source parameters can be predicted and then used for hazard prediction and emergency response planning in real time.

There are many approaches to source estimation. Rao (2007) provides a summary of some of the methods, categorizing the approaches into broadly two methods: Forward modeling methods and Backward modeling methods. Some of these approaches have been implemented using the SCIPUFF model. The Aerodyne Inverse Modeling System (AIMS) uses the tangent-linear numerical adjoint of SCIPUFF combined with a minimization algorithm to predict the number of sources, locations and other information, as detailed in Albo et al (2011). AIMS does not need the initial estimate for the source parameters as an input, and has the advantage of integrating data from both mobile and stationary sensors.

Annunzio et al. (2012) adopted the Lagrangian entity backtracking approach for the source estimation. This method analyzes the state of larger contaminant-filled entities as opposed to the smaller fluid parcels. There are a couple of advantages of using this method. Firstly it does not require the same kind of meteorological and concentration data as the Lagrangian parcel backtracking. Secondly, the pollutant puffs can be superimposed to predict the concentration field and the state of each contaminant puff can then be extrapolated backward to predict the source location.

The Urban Dispersion Model which has been developed by the UK Defense Science Technology Laboratory (DSTL) combines Gaussian Puff modeling with empirically deduced mixing and entrainment approximations. The source term parameters can be estimated by using the Markov Chain Monte Carlo (MCMC) sampling method in conjunction with UDM. These parameters can be refined by using the finite element CFD model. Bayesian probability theory is used in conjunction with adjoint advection-diffusion equation and MCMC sampling, for source determination.

In this paper, we will be presenting the method and results for source estimation using the adjoint transport equation with SCIPUFF. The advantage of this approach is that the source estimation model is incorporated in the SCIPUFF model and does not need any additional model or analysis tool.

2 SCIPUFF MODEL

2.1 FORWARD MODEL

SCIPUFF is an atmospheric dispersion model with a wide range of application. The turbulent diffusion parameterization is based on second-order turbulence closure theory, which relates the dispersion rate to velocity fluctuation statistics. In addition to the average concentration value, the closure model provides a prediction of the statistical variance in the concentration field resulting from the random fluctuations in the wind field. The variance is used to estimate a probability distribution for the predicted value, using the clipped normal function. SCIPUFF uses a collection of Gaussian puffs to represent an arbitrary three-dimensional, time-dependent concentration field, and incorporates an efficient scheme for splitting and merging puffs. Wind shear effects are accurately modeled, and puffs are split when they grow too large for single point meteorology to be representative. These techniques allow the puff model to describe complex flow effects on dispersion, such as terrain-driven circulations

The concentration field in SCIPUFF is described using the sum of contributions from a collection of three-dimensional puffs

$$c(\boldsymbol{x}) = \sum_{\alpha} c^{(\alpha)}(\boldsymbol{x}) = \sum_{\alpha} Q^{(\alpha)} G^{(\alpha)}(\boldsymbol{x}) \tag{2.1}$$

where the sum is taken over all the contributing puffs denoted by superscript α, and $G^{(\alpha)}$ is the spatial Gaussian distribution of the puff given by

$$G^{(\alpha)}(\boldsymbol{x}) = \frac{1}{V} \exp\left[-\frac{1}{2} \left(\sigma_{ij}^{(\alpha)}\right)^{-1} \left(x_i - \overline{x}_i^{(\alpha)}\right)\left(x_j - \overline{x}_j^{(\alpha)}\right) \right] \tag{2.2}$$

where the puff volume V, is

$$V = (2\pi)^{3/2} \left\| \sigma^{(\alpha)} \right\|^{1/2} \tag{2.3}$$

and $\| \ \|$ denotes the determinant.

The spatial moments in (2.1) and (2.2) are given by the integral over all space as

Zeroth moment- mass	$Q^{(\alpha)} = \int_v c^{(\alpha)} \, dV$	(2.4)
First moment- centroid	$Q^{(\alpha)} \overline{x}_i^{(\alpha)} = \int_v c^{(\alpha)} x_i \, dV$	(2.5)
Second moment- spread	$Q^{(\alpha)} \sigma_{ij}^{(\alpha)} = \int_v c^{(\alpha)} (x_i - \overline{x}_i^{(\alpha)})(x_j - \overline{x}_j^{(\alpha)}) \, dV$	(2.6)

The model is advanced in time by solving ordinary differential equations for the puff moments. (Sykes et al., 1993). These equations are obtained from the advection-diffusion

equation for a scalar quantity in an incompressible flow field. The advection-diffusion equation is

$$\frac{\partial c}{\partial t}+\frac{\partial}{\partial x_i}\left(u_i c\right)=k\nabla^2 c+R \tag{2.4}$$

where $u_i\left(x_i,t\right)$ is the turbulent velocity field, k is the molecular diffusivity, and R represents the source terms.

2.2 ADJOINT MODEL

The source estimation capability in SCIPUFF is based on the adjoint of the dispersion model equations, which gives a reverse diffusion calculation indicating the location where material may have been released in order to result in the observed concentration measurements. We first introduce the definition of the adjoint and the relationship between sensor concentration measurements and source terms. The transport and dispersion of a passive scalar is given by the advection-diffusion equation, (2.4)

The left hand side can be written as a linear operator, L, acting on the concentration field, where

$$L\left(c\right)=\frac{\partial c}{\partial t}+\frac{\partial}{\partial x_i}\left(u_i c\right)-k\nabla^2 c \tag{2.5}$$

The adjoint of L is defined in terms of an inner product, such that the adjoint satisfies the relation

$$\left\langle L\left(c\right),c^*\right\rangle=\left\langle c,L^*\left(c^*\right)\right\rangle \tag{2.6}$$

for any fields c and c^*. The angle brackets denote an inner product between two fields, and we define the inner product as the integral over all space and time.

$$\langle f, g \rangle = \int f\, g\, dV\, dt \tag{2.7}$$

With this definition of the inner product, the adjoint of the advection-diffusion operator,(2.5) , can be shown to be

$$L^*(c^*) = -\frac{\partial c^*}{\partial t} - \frac{\partial}{\partial x_i}(u_i c^*) - k\nabla^2 c^* \tag{2.8}$$

The adjoint is very similar to the forward transport operator, and for an incompressible velocity field, it simply represents a reversal of the time variable and also of the velocity field. Note that the diffusion term is not reversed, so the adjoint does not reverse the diffusion process. The relationship between sensor measurements and source terms is obtained through the inner product definition. A very specific requirement for use of the adjoint is linearity, both of the transport operator and also the sensor measurements. We represent a sensor output as

$$d = \int c(\boldsymbol{x},t)\hat{R}(\boldsymbol{x},t)\, dV\, dt \tag{2.9}$$

where d is the output value of the sensor, and $\hat{R}$ is the sensor response function. This is the most general linear sensor description, and shows the sensor as a weighted integral of the concentration field. The sensor response will generally be localized in space and time, but the formalism accommodates any linear response.

The notation for the sensor response function is chosen to suggest the adjoint, and this is now clear when we solve the adjoint dispersion equation with the sensor response as the source term. We solve

$$L^*(c^*) = \hat{R}(\boldsymbol{x},t) \tag{2.10}$$

to obtain the adjoint concentration field, c^*. The sensor data value in (2.9) can now be written as

$$d = \langle c, L^*(c^*) \rangle \tag{2.11}$$

and the definition of the adjoint in (2.6) allows us to rewrite this as

$$d = \langle L(c), c^* \rangle \tag{2.12}$$

or

$$d = \langle R, c^* \rangle \tag{2.13}$$

where R is the source term. The important property of the adjoint is that it gives a direct predictor for the sensor data value for any source term, R. The adjoint is effectively a receptor model, since it only gives information about the concentration field that the sensor would experience for a release from any location. This contrasts with the forward dispersion model, which gives information about the concentration everywhere for a release from a specific location.

The adjoint model can be validated by running the model with the same release mass as the forward model. The concentration at a receptor after a certain time should match the adjoint concentrations from the receptor after the same reverse time period at the forward or actual source location. Based on the sampler networks from two experimental studies viz. Fusion Field Trail 2007 (FFT07) [Platt N. and Deriggi D., 2010] and the European Tracer experiment, 1996 (ETEX) [Mosca et al., 1997], the comparative results for the forward model concentrations with the adjoint model concentrations are given below. Figure 1(a) shows the concentration measurements at some of the sensors from a network of 100 sensors arranged on a regular grid for FFT07. The release is made from the actual source location and concentrations measurements are made at sensor 86 after 20s. Figure 1(b) shows the adjoint concentration at the actual source location after 20s when there is a same amount of release from sensor 86. Similarly the forward and adjoint concentration plots are shown in Figure 1(c), (d) after 60s for sensor 25 and in Figure 1(e), (f) after 90s for sensor 4. The concentration values and the ratio for the FFT07 forward and adjoint model are listed in Table 1 and show that the ratios for these cases are close to 1.

Table 1: Forward and adjoint concentration ratios for FFT07

Time(s)	Sampler ID	Concentration (kg/m3)		Ratio
		Forward	Adjoint	
20.0	86	1.4987e-07	1.5701e-07	0.954
60.0	25	2.6037e-06	2.7127e-06	0.960
90.0	04	1.2119e-06	1.1767e-06	1.030

The sensor network for ETEX consisted of 168 sensors over a domain of approximately 1800 sq. km. The forward and adjoint model concentration comparison plots are shown in Figure 2(a-f) for an instantaneous release mass of 340 kg of SF6. Figure 2(a), (b) shows the forward and adjoint concentrations for sensor 108 after 12 hrs. Figure 2(c), (d) are concentrations for sensor 30 after 30 hrs. and Figure 2(e), (f) are concentrations for sensor 129 after 60 hrs. Table 2 lists the concentrations values and their ratios. For these sensors, the adjoint concentration values are also within 10% of the forward concentrations.

Table 2: Forward and adjoint concentration ratios for ETEX

Time(Hr)	Sampler ID	Concentration(kg/m3)		Ratio
		Forward	Adjoint	
12	108	4.78E-10	4.674E-10	0.97
30	30	2.61E-12	2.45E-12	0.94
60	129	4.25E-12	4.47E-12	0.95

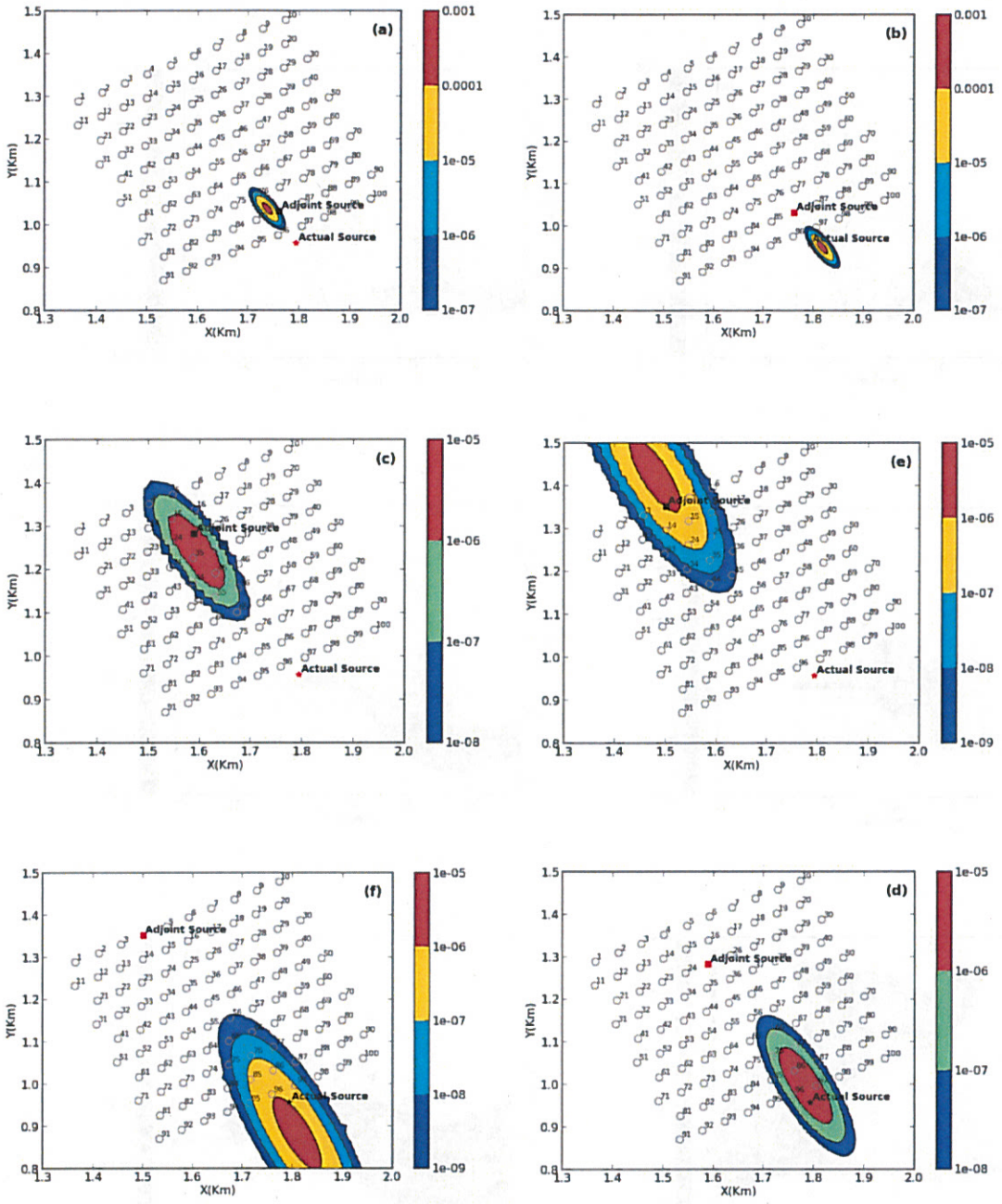

Figure 1: Forward and adjoint concentrations (kg/m3) for FFT07 at (a,b) 20s, (c,d) 60s,

(e,f) 90s based on release 1 of Trial 71.

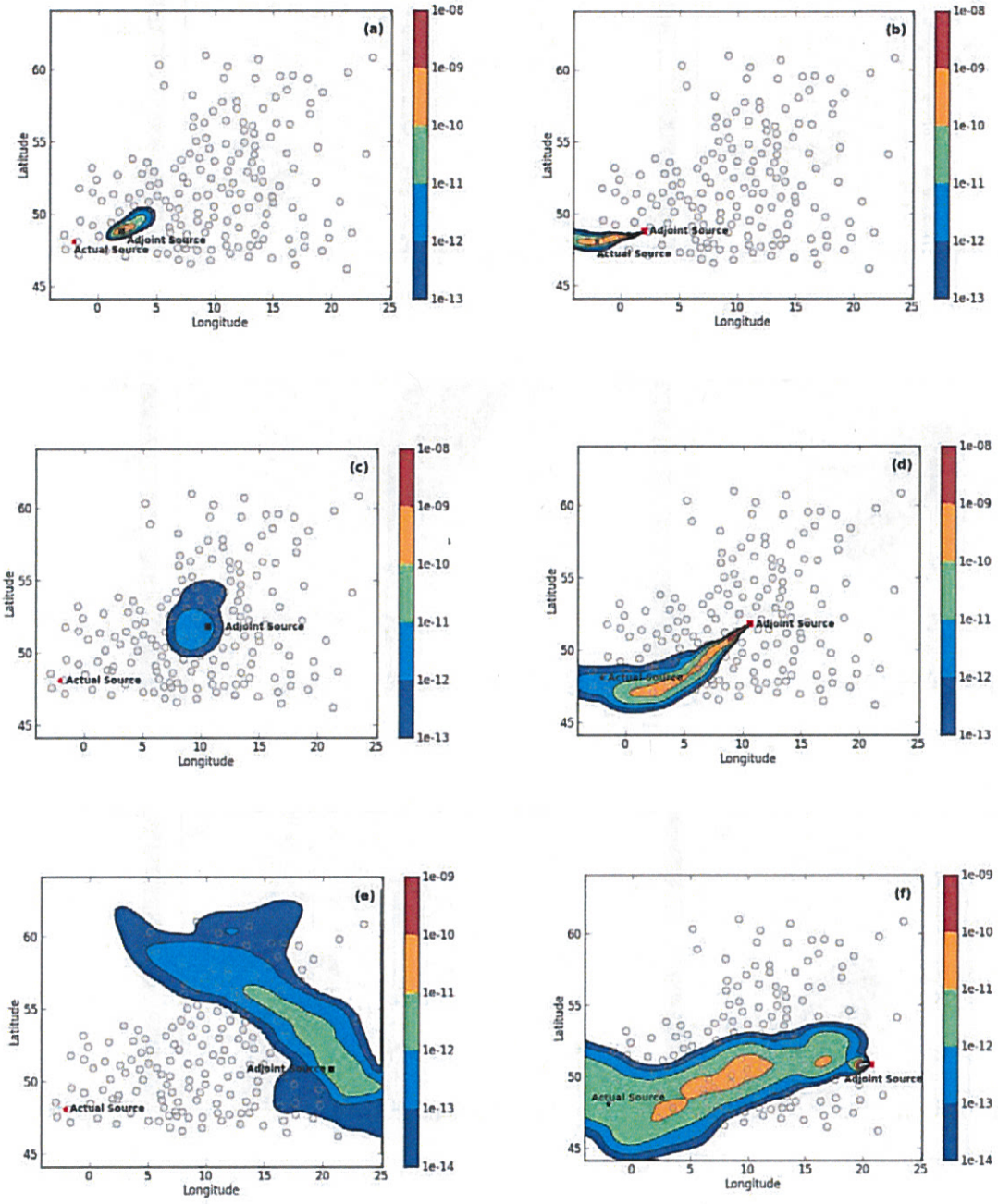

Figure 2: Forward and adjoint concentrations (kg/m^3) for ETEX

2.3 SOURCE TERM ESTIMATION

2.3.1 Release Estimate

The adjoint relationship in (2.13) gives the model-predicted data value in terms of the release specification and the adjoint concentration. If the release is normalized by the release mass, or release mass rate for a continuous release, we can write (2.13) as

$$d = Q\left\langle \hat{R}, c^* \right\rangle \tag{2.14}$$

where, Q is the release mass and $\hat{R}(\boldsymbol{x},t)$ defines the geometry and location of the release. This relation can be rearranged to give a predicted release mass, using the observed data value, d, so that

$$Q = \frac{d}{\left\langle \hat{R}, c^* \right\rangle} \tag{2.15}$$

Note that we assume $d > 0$ in order to obtain a non-zero release mass estimate, and we consider only non-zero sensor data in this section; non-triggered or null sensor data is considered in the next section. We refer to such data as "triggered", and the adjoint field from a triggered sensor is denoted by c^*. The two simple release geometries that are implemented in the estimation routines are instantaneous and continuous point sources. These two geometries are defined as

$$\hat{R}_{inst}(\boldsymbol{x},t;\boldsymbol{x}_R,t_R) = \delta(\boldsymbol{x}-\boldsymbol{x}_R)\delta(t-t_R) \tag{2.16}$$

and

$$\hat{R}_{cont}(\boldsymbol{x},t;\boldsymbol{x}_R,t_R,t_{dur}) = \delta(\boldsymbol{x}-\boldsymbol{x}_R)\left[H(t-t_R)-H(t-t_R-t_{dur})\right] \tag{2.17}$$

where x_R is the release location, t_R is the release time and t_{dur} is the duration of the continuous release. The size of the source is generally not a significant factor in determining the sensor

value, as long as the sensor is reasonably distant from the source, so the point location is used to simplify the release mass estimate. For the two release geometries, the mass estimate becomes

$$Q_{inst}(\boldsymbol{x}_R, t_R) = \frac{d}{c^*(\boldsymbol{x}_R, t_R)} \tag{2.18}$$

and

$$Q_{cont}(\boldsymbol{x}_R, t_R, t_{dur}) = \frac{d}{\int_{t_R}^{t_R + t_{dur}} c^*(\boldsymbol{x}_R, t)\, dt} \tag{2.19}$$

The instantaneous release estimate uses the adjoint concentration, which can be generated from the stored puff file in either horizontal or vertical slices. The continuous release estimate requires a time-integrated concentration value, and this is obtained by differencing the surface dosage field at the two times defining the integration limits. Note that continuous release estimates are therefore limited to the two-dimensional dosage field.

Note that every sensor measurement, d_i, can be used to generate an adjoint concentration field, c_i^*, and hence defines a release mass estimate, Q_i, for any source geometry and for all release parameters, which are location, time, and duration for the continuous release. The release estimate uses the mean adjoint concentration, $\overline{c}_i^*$, in (2.15) to define the release mass and therefore effectively assumes that the mean forward concentration is the prediction for the sensor measurement, i.e., it is a deterministic estimate. We note that the mean concentration is not a good predictor in situations where there is a large uncertainty in the concentration value. This is always the case in the edges of a plume or cloud, but we will assume that the values in the plume center are relatively certain.

The basis of the source estimation algorithm is to search over the release parameter space to determine where the adjoint fields from multiple sensor measurements define a consistent release mass. If such a point exists, where all the mass estimates are the same, then it implies that all the sensor measurements would be perfectly predicted from that particular release. In practice, of course, we do not achieve perfect agreement, and we therefore search for a

maximum in an empirical measure of the consistency. One could use a measure of the overall spread or range of the mass estimates, but this type of gross measure is easily dominated by a small number of outliers. We have found that a measure that counts all adjoint results with roughly equal weight provides a more robust result. We construct such a measure by considering all unordered pairs of mass estimates. For each pair of values, Q_i and Q_j, where $i \neq j$, we define the ratio

$$r_{ij} = \frac{Q_i}{Q_j} \tag{2.20}$$

where we choose the indices such that $Q_i \leq Q_j$, i.e., $0 \leq r_{ij} \leq 1$. If there are N_{trig} sensor measurements, then we will have $N_{trig}\left(N_{trig}-1\right)/2$ pair ratios. A simple initial estimator is therefore

$$\bar{r} = \frac{2}{N_{trig}\left(N_{trig}-1\right)}\sum_{i\neq j} r_{ij} \tag{2.21}$$

which necessarily provides a value between zero and one. The estimate in (2.21) was found to require additional weighting to account for highly uncertain mass estimates in the remote edges of the plume, which occasionally produced anomalously high values of $\bar{r}$. We therefore use the predicted probability of non-zero adjoint concentrations, and generalize the estimate to give

$$\bar{r} = \frac{2}{N_{trig}\left(N_{trig}-1\right)}\sum_{i\neq j} w_{ij} r_{ij} \tag{2.22}$$

where $w_{ij} = \max\left(\Pr\left(\left\langle \hat{R}, c_i^* \right\rangle > 0\right), \Pr\left(\left\langle \hat{R}, c_j^* \right\rangle > 0\right)\right)$, which eliminates the contribution when both values are extremely uncertain.

2.3.2 Non-triggered Sensor Measurements

Sensors recording no measurable concentration can also provide information about the release location, although they cannot be used to determine the release mass if we use a data

value, d, of zero in (2.15). A non-triggered sensor reading provides an upper bound on the release mass, i.e., the release was not sufficiently large mass to register a response at the sensor. We implement a model for non-triggered sensors using a threshold response level, d_{min}, which must be greater than or equal to zero. The interpretation in terms of release mass then becomes

$$Q \le \frac{d_{\min}}{\left\langle \hat{R}, n^* \right\rangle} \tag{2.23}$$

for the adjoint field, n^*, resulting from a non-triggered sensor.

The information from the non-triggered sensor data values is used to provide a further multiplicative weight to the ratio value, r_{ij}, in (2.22). For each non-zero, or triggered, sensor value, we define a non-triggered-based weight as

$$w_i^N < \prod_{j=1}^{N_{null}} \Pr\left(Q_i \le \frac{d_{\min}}{\left\langle \hat{R}, n_j^* \right\rangle} \right) \tag{2.24}$$

i.e., the combined probability that the mass estimate is below the threshold requirement of all the non-triggered sensors. Note that this weight is defined in terms of a probabilistic estimate from the adjoint field, since we expect the non-triggered measurements to be either in the edges or outside the plume, and in these regions a deterministic estimate is inappropriate. The expression for the non-triggered weight can be rewritten as

$$w_i^N < \prod_{j=1}^{N_{null}} \Pr\left(\left\langle \hat{R}, n_j^* \right\rangle \le \frac{d_{\min}}{Q_i} \right) \tag{2.25}$$

The weights in (2.22) are extended to include the weighting from the non-triggered sensors, so that

$$w_{ij} = \sqrt{w_i^N \, w_j^N} \max\left(\gamma_i, \gamma_j\right) \tag{2.26}$$

where $\gamma_i = \Pr\left(\left\langle \hat{R}, c_i^* \right\rangle > 0\right)$ for the adjoint field from a triggered sensor.

2.4 FAST SEARCH

Source estimation is based on finding the maximum value of the empirical location function, $\bar{r}$ given by (2.22) which is defined for all space and time. Time and duration are discretized on the basis of saved times using interval halving. SCIPUFF uses adaptive grids for dosage and concentration grids; Figure 3 illustrates an adaptive grid with three levels of refinement. C1-C4 grid cells are on the top (zero) level. The cell C4 is further refined to C5-C8 cells, which are on the first level. Similarly, the C5 cell is again refined to the second level C9-C12.

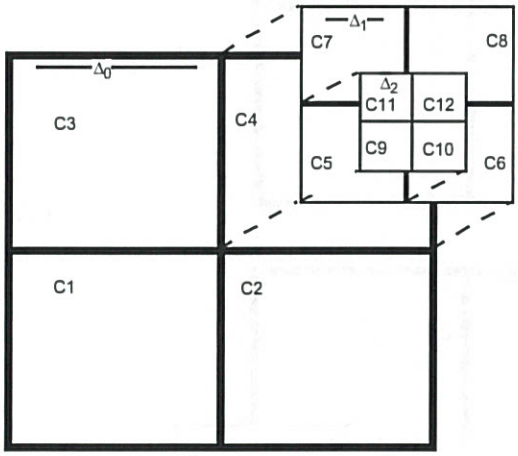

Figure 3: Schematic diagram of concentration and dosage adaptive grid in SCIPUFF with three levels

Each adjoint material uses its own adaptive grid and this is shown for two material A and B in Figure 4(a) and Figure 4(b). For the spatial search, the adaptive grids for different adjoint materials are combined and the function $\bar{r}$ is calculated for each cell of the combined grid. Figure 5(a) shows combined for material A and material B. This search can be very time consuming since there may be a large number of cells, so a method based on wavelet

methodology is used to speed up the search over large spatial grids. The concentration or dosage data is averaged on to coarser or upper level grid cells. This technique for averaging the cell values onto coarser levels is referred to as "rezoning" in SCIPUFF and the schematic diagram in Figure 5(b) shows the cells after rezoning of the combined grid for Material A and Material B. The search is conducted over the rezoned cells for the upper level and based on the search results the rezoned cell with the highest value is selected and the search is continued on the finer rezoned cells for the selected grid cell. This results in extremely efficient search over large grids with more than 25000 cells.

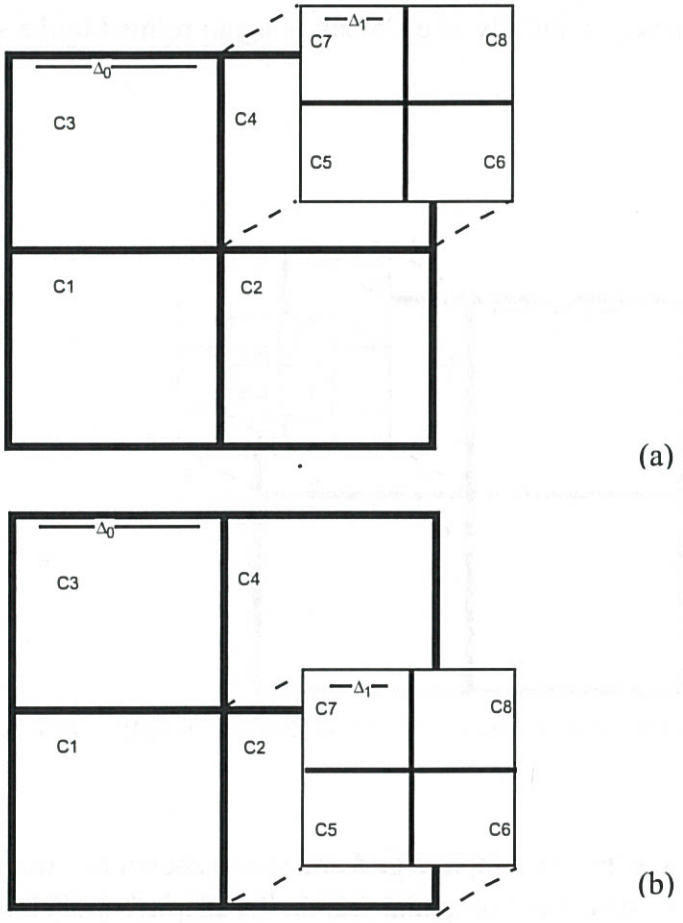

Figure 4: Schematic diagram of concentration and dosage adaptive grid for (a) Material A and (b) Material B

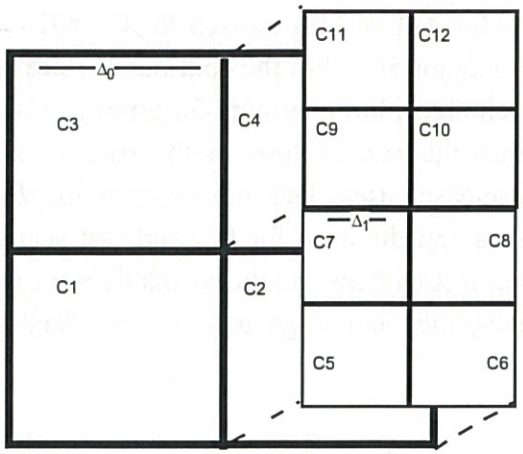

(a)

Rezone

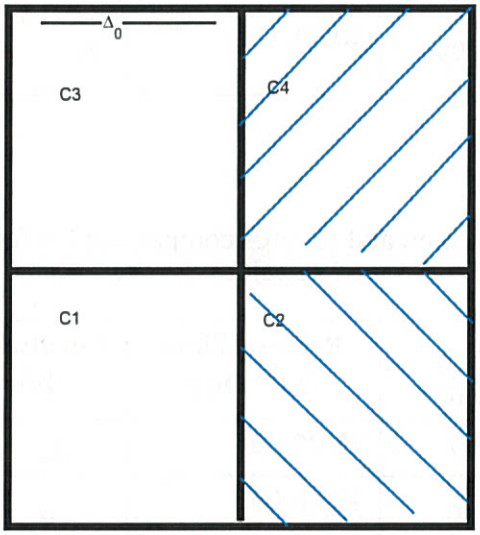

(b)

Figure 5: Schematic diagram of combined grid for Material A and Material B (a) before and (b) after rezone.

Table 3 shows the timing and results for full and fast search for Case016 of FFT07. The speedup in this case is approximately a factor of 4. For the continuous release case of ETEX, the speedup from using the Fast search algorithm is around 50 times as seen from Table 4. Table 3 and Table 4 also show that the results from both searches are identical for instantaneous as well as continuous release cases. The maximum source location function values in the domain at different times and duration for full and fast search are shown in Figure 6 and Figure 7. From the figures it is evident that the search over the temporal domain and duration differ initially. However, they converge to the same final source location function value.

Table 3: Comparison of full search vs fast search source term estimation results and timings for Case016 of FFT07

	Source Location		**Release Time (21st Sept)**	**Run Time**
	Easting	**Northing**		
Observed	331.794	4439.957	10:04:00	
Full Search	331.814	4439.994	10:04:11	16s
Fast Search	331.814	4439.994	10:04:11	4s

Table 4: ETEX source term estimation and timings comparison for full search vs fast search

	Source Location		**Release Time (23rd Oct)**	**Duration (Hr)**	**Run Time**
	Longitude	**Latitude**			
Observed	-2.017	48.07	16:00:00	12	
Full Search	-2.567	47.80	23:00:00	08	4 hr 9 min
Fast Search	-2.567	47.80	23:00:00	08	5 min 20s

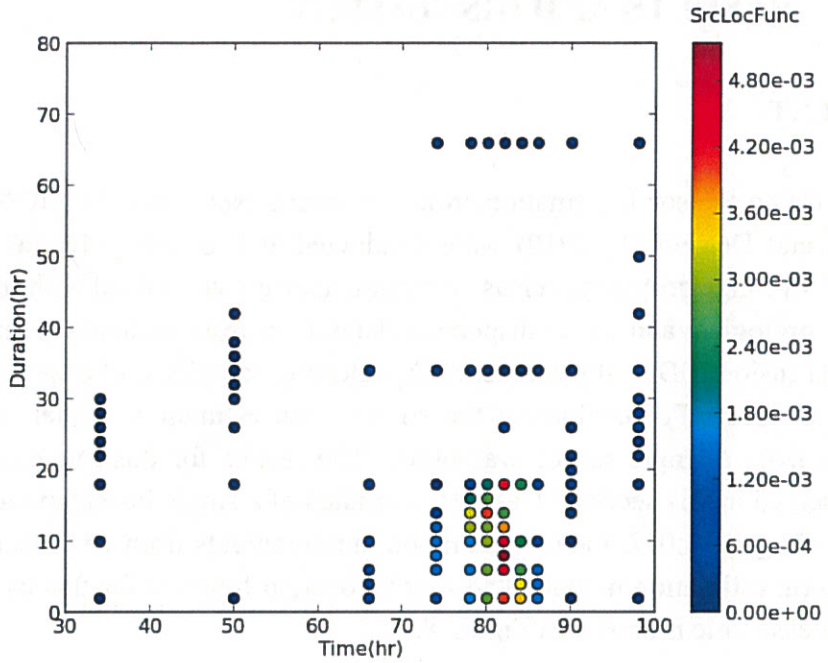

Figure 6: Source location function at different time and duration using full search for ETEX

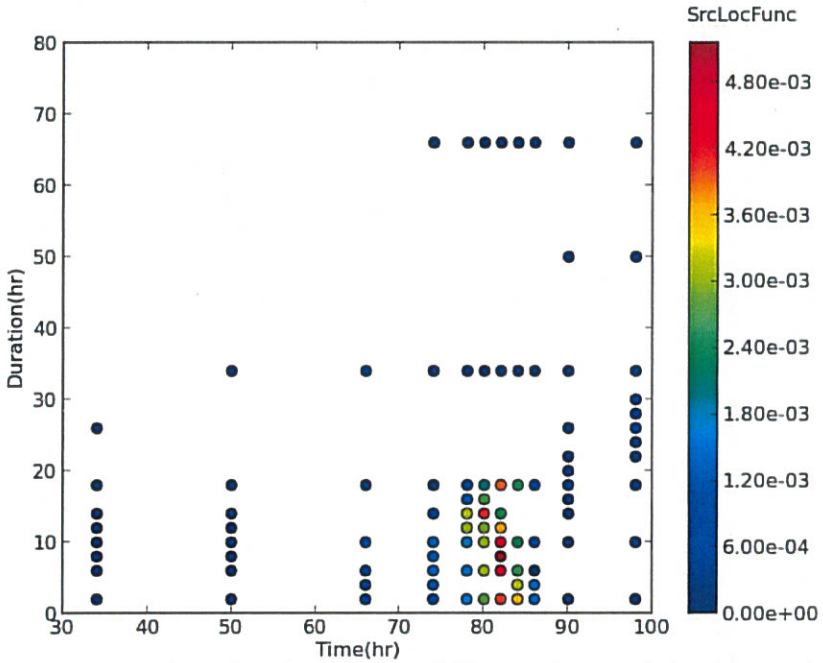

Figure 7: Source location function at different time and duration using fast search for ETEX

3 RESULTS AND DISCUSSION

3.1 FFT07 EXPERIMENT

In September 2007, the FUsing Sensor Information from Observing Networks (FUSION) Field Trial tests (Platt N. and Deriggi D., 2010) were conducted at U.S. Army Dugway Proving Ground. These short-range propylene release experiments were conducted with the purpose of creating a meteorological and tracer dispersion dataset for testing chemical and biological (CB) sensor data fusion (SDF) algorithms. A high density sampler grid covering a 500m by 500m area was used. For evaluating the source term estimation model, an instantaneous release case from a single source was used. The results for this test case, Case016 of FFT07, is presented in this section. Case016 consisted of a single instantaneous release with a mass of 0.698 kg at 10:04Z and concentration measurements from 16 sensors were used for the source term estimation model. The source location function for this case relative to the estimated release time is shown in Figure 8.

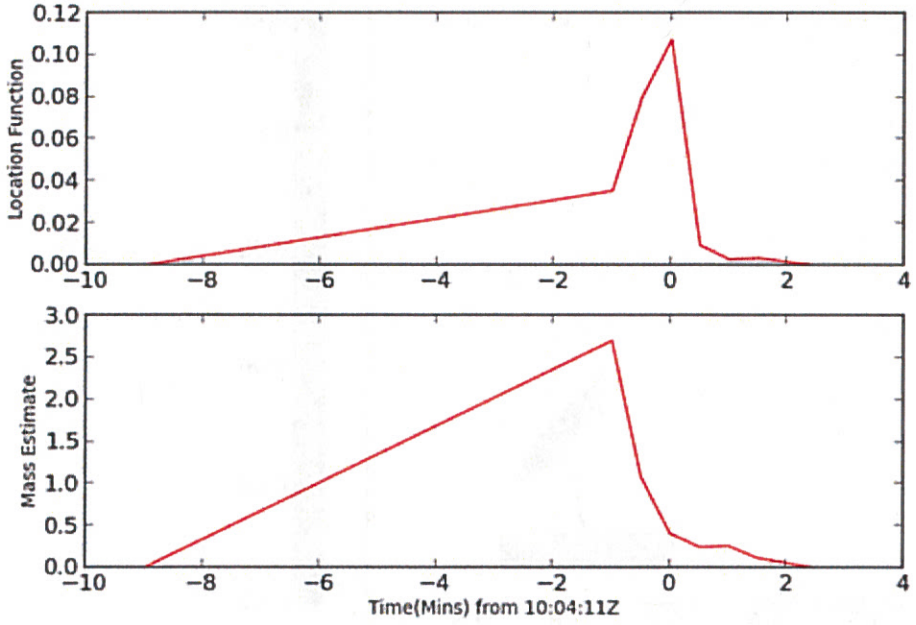

Figure 8: Location function and estimated mass versus time for Case016 of the FFT07 experiment.

Based on the maximum source location function, the estimated release time is 10:04:11 and the release mass is 0.409 kg. The sensor and estimated source locations for Case016 is shown in Figure 9. The estimated release time is the same as the actual release time and the release mass is within a factor of 2; the source location is within 42m of the actual source.

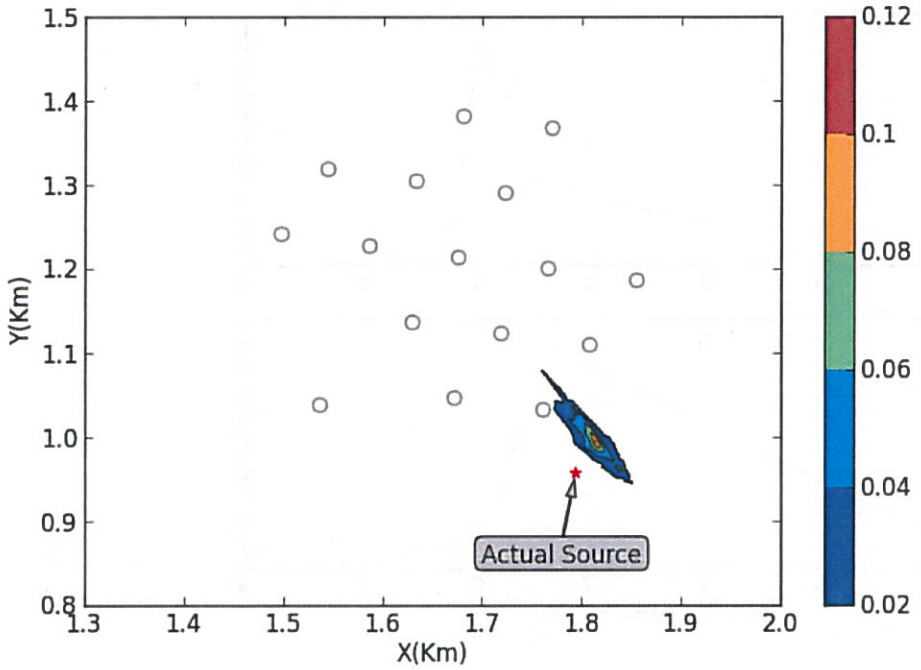

Figure 9: Contour plots for instantaneous source location function with estimated and actual source location for FFT07 Case 16 release.

3.2 EUROPEAN TRACER EXPERIMENT

The second experiment is the European Tracer Experiment (ETEX) (Mosca et al., 1997). In this study, an inert tracer was released for 12 hours at an average rate of 7.95 g/s. The evolution of the tracer cloud was measured for a period of 72 hours (from the beginning of the release) with a sampling network of 168 sites. The meteorological input to SCIPUFF was the uninitialized, gridded analysis supplied by the European Centre of Medium Range Weather Forecasts (ECMWF). Since this did not include boundary layer depth and surface heat flux (parameters required to define turbulence profiles), SCIPUFF's boundary layer calculation based on a surface energy balance method was utilized assuming no cloud cover. Uniform surface characteristics were also assumed, with values of 5 cm for roughness, 0.6 for Bowen ratio and 0.16 for surface albedo. These values are typical of mid-latitude rural terrain, but clearly cannot represent the detailed variations over the dispersion domain.

Additionally, turbulence input for the second-order closure model was specified as two separate populations, representing the planetary boundary layer eddies and the larger scale contribution. The large-scale turbulence represents the mesoscale fluctuations, and is based on the work of Gifford (1988). The source location function and mass estimate variation with time and the change of location function with release duration are shown in Figure 10. Figure 11 shows the sensor used as input to the adjoint model.

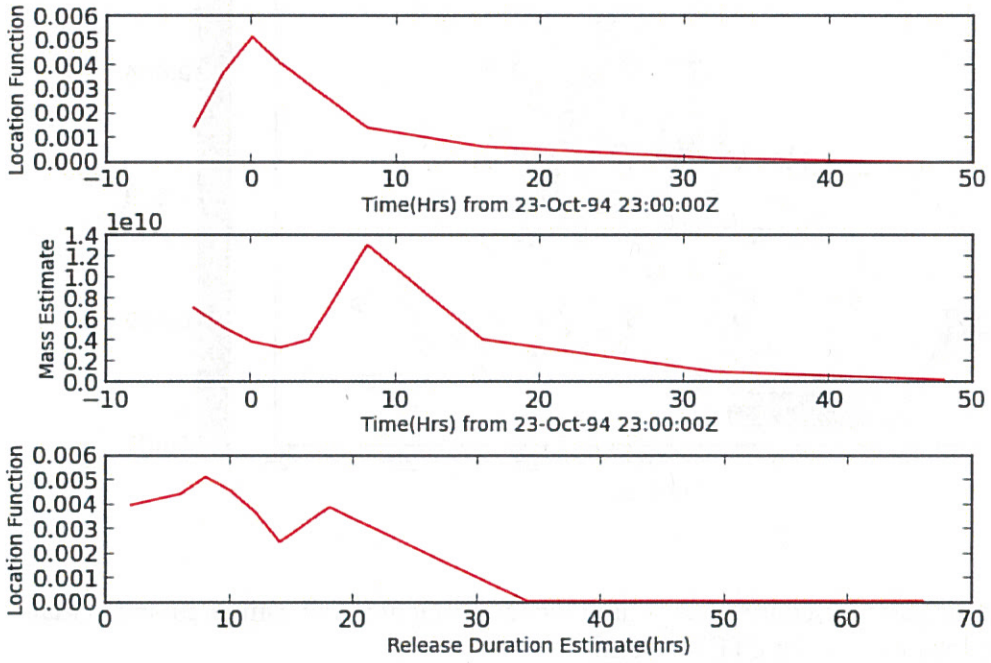

Figure 10: Location function, estimated mass and release duration for ETEX

The contour plots in Figure 11 shows the source location function at the estimated release time; the actual source, predicted source and the sensor locations are also shown on Figure 11. The estimated source location is (-2.567,47.8) compared to the actual release location of (-2.01,48.06) and predicted release duration is 8 hrs compared to the actual duration of 12

hrs. The predicted release time is '23-Oct-94', '23:00:00Z' compared to '23-Oct-94', '16:00:00Z'

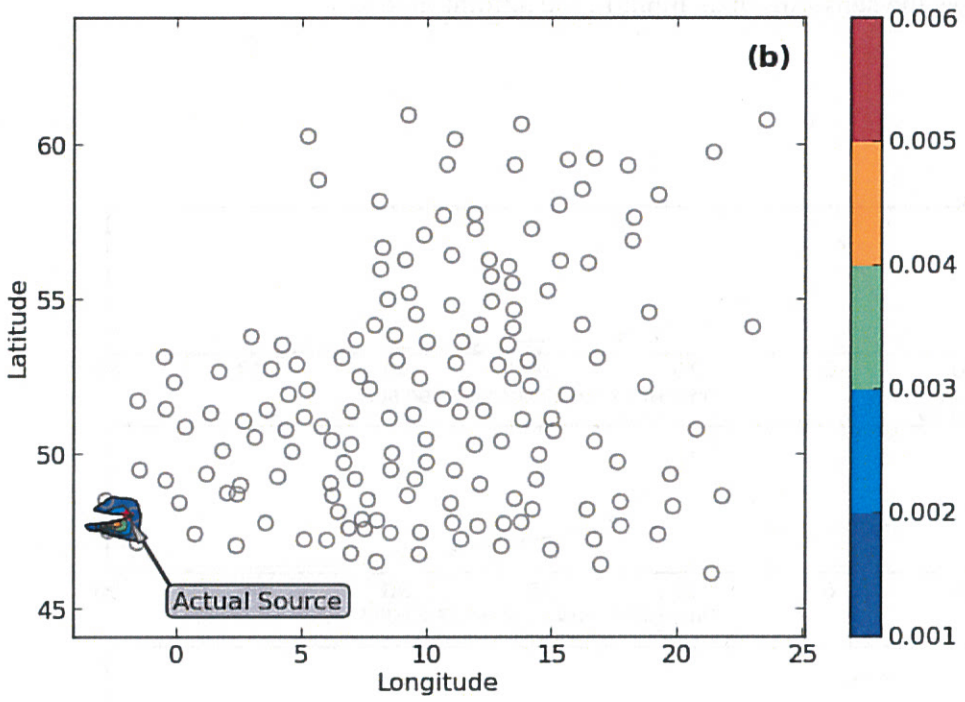

Figure 11: Contour plots for continuous source location function and estimated and actual source location for the ETEX release.

4 CONCLUSION

The adjoint SCIPUFF model can be used for the estimation of source parameters such as the source location, source strength, source type and release time and duration for a single source using sensor data from a network of sensors. Using the fast search, the source term estimation

algorithm provides results in a reasonable time and can be incorporated into real time hazard prediction and emergency planning.

The methodology is heuristic in the sense that the adjoint of the turbulence closure equations has not been formally derived, but the adjoint relationship has been shown to hold within numerical calculation differences over long range transport for several days. The source estimation procedure has been demonstrated with reasonable success using experimental data on a range of scales.

Finally, we note that the deterministic source term estimation model is based the mean adjoint concentration field and assumes that there is no significant uncertainty due to the turbulent transport. However, if there are significant uncertainties due to uncertainties in the measurements or meteorology the mean concentration is a poor estimate of what a real sensor might experience, so the mean adjoint concentration gives an equally poor estimate of the release mass. In these situations, it may be more appropriate to use the conditional average concentration for a probabilistic estimate. Also, for general application of the source estimation model, the user has to specify the source type as instantaneous or continuous as the model cannot automatically determine the source type.

5 REFERENCES

Albo, S. E., Oluwole, O. O., Miake-Lye, R. C., 2011. The Aerodyne Inverse Modeling System (AIMS): Source estimation applied to the FFT 07 experiment and to simulated mobile sensor data, *Atmos. Env.*,**45**, 6085-6092.

Annunzio A.J, Andrew J. , Haupt S.E., Young G.S., 2012. Utilizing state estimation to determine the source location for a contaminant, *Atmos. Env.*, **46**, 580-589

Biltoft, C. A., 1997: Phase I of Defense Special Weapons Agency Transport and Dispersion Model Validation, DPG-FR-97-058, U.S. Army Dugway Proving Ground, Dugway, Utah.

Rao, K.S., 2007. Source Estimation Methods for Atmospheric Dispersion., *Atmos. Env.*, **41**, 6964-6973

Hanna, S., S. Dharmavaram, J. Zhang, I. Sykes, H. Witlox, S. Khajehnajafi. and K. Koslan (2008). "Comparison of six widely-used gas dispersion ,models for three recent chlorine railcar accidents." Process Safety Progress, 27, 248-259.

Haupt, S.E., Haupt, R.L., Young, G.S., 2011. A mixed integer genetic algorithm used in biological and chemical defense applications. *Soft Computing*, **15**, 51-59.

Long, K.J., Haupt, S.E., Young, G.S., 2010. Assessing sensitivity of source term estimation. *Atmos. Env.*, **44**, 1558-1567.

Lushi, E., Stockie, J.M., 2009. An inverse Gaussian plume approach for estimating atmospheric pollutant emissions from multiple point sources. *Atmos. Env.*, **44**, 1097-1107.

Mosca, S., Graziani, G., Klug, W., Bellasio R. and Bianconi R. (1997), "ATMES-II - Evaluation of long-range disperions models using 1st ETEX release data: Volume 1", JRC-Environment Institute.

Platt, N. and Deriggi, D., 2010. Comparative investigation of source term estimation algorithms using fusion field trial 2007 data, 8th Conference on Artificial Intelligence Applications to Environmental Sciences at AMS Annual Meeting, Atlanta, GA.

Platt, N., Warner, S., Nunes, S.M., 2008. Evaluation plan for comparative investigation of source term estimation algorithms using Fusion Field Trial 2007 data, *Croatian Meteorological Journal* **43** (1).

Sykes, R. I., S. F. Parker, D.S. Henn, and W.S. Lewellen (1993). "Numerical simulation of ANATEX tracer data using a turbulence closure model for long-range dispersion." J. Appl. Met., 32, 929-947.

Sykes, R.I., Gabruk, R.S., 1997. A second-order closure model for the effect of averaging time on turbulent plume dispersion. *J. Appl. Met.,* **36** (8).

Sykes, R.I., Lewellen, W.S., Parker, S.F., 1985. A Gaussian plume model of atmospheric dispersion based on second-order closure. *J. Clim. and Appl. Met.*, **25**.

Yee, E., Kosteniuk P. R., and Bowers J. F.,1998. A Study of Concentration Fluctuations in Instantaneous Clouds Dispersing in the Atmospheric Surface Layer for Relative Turbulent Diffusion: Basic Descriptive Statistics, *Boundary-Layer Meteorology*, **87**, 409-457